

COMPUTATIONAL FLUID DYNAMICS FOR WIND ENGINEERING

R. PANNEER SELVAM



WILEY Blackwell

Table of Contents

[Cover](#)

[Title Page](#)

[Copyright Page](#)

[Preface](#)

[References](#)

[1 Introduction](#)

[1.1 Brief Review of Steps in CFD Modeling](#)

[1.2 CFD for Wind Engineering or Computational Wind Engineering](#)

[References](#)

[2 Introduction to Fluid Mechanics](#)

[2.1 Navier-Stokes Equations](#)

[2.2 Governing Equations for Compressible Newtonian Flow](#)

[2.3 Definition of Convection and Diffusion](#)

[2.4 Derivation of Bernoulli Equations](#)

[2.5 Velocity Computation in an Incompressible, Irrotational, Steady, and Inviscid Flow](#)

[2.6 Nondimensional NS Equations](#)

[2.7 Properties of Fluids](#)

[2.8 Solution of Linear and Nonlinear Equations](#)

[2.9 Laminar and Turbulent Flow](#)

[2.10 Velocity Spectrum and Spectrum Considered by Different Turbulence Models](#)

[2.11 Turbulence Modeling](#)

[2.12 Law of the Wall](#)

[2.13 Boundary Layer Depth Estimation](#)

[2.14 Chapter Outcome](#)

[Problems](#)

[References](#)

[3 Finite Difference Method](#)

[3.1 Introduction to Finite Difference Method](#)

[3.2 Example for 2D Potential Problem and Solution of Simultaneous Equations-Direct and Iterative Methods](#)

[3.3 Finite Difference Method of Approximating the Partial Differential Equation](#)

[3.4 Unsteady Problem-Explicit and Implicit Solution for the Wave Equation](#)

[3.5 Solution of the Incompressible Navier-Stokes \(NS\) Equations](#)

[3.6 Storage of Variables in Staggered and Nonstaggered Grid Systems](#)

[3.7 Node and Cell-Centered Storage Locations](#)

[3.8 Structured and Unstructured Grid Systems](#)

[3.9 Variable Storage Methods](#)

[3.10 Practical Comments for Solving the NS equation](#)

[3.11 Chapter Outcome](#)

[Problems](#)

[References](#)

[4 Introduction to Wind Engineering](#)

[4.1 Wind Velocity Profile Due to Ground Roughness and Height](#)

[4.2 Topographic Effect on Wind Speed](#)

[4.3 Wind Speed and Wind Pressure](#)

[4.4 Wind and Structure Interaction](#)

[4.5 Opening in the Building](#)

[4.6 Phenomena not Considered by the ASCE 7-16](#)

[4.7 ASCE 7-16 on Method of Calculating Wind Load](#)

[References](#)

[5 CFD for Turbulent Flow](#)

[5.1 Mean and Peak Pressure Coefficients from ASCE 7-16 and Need for CFD](#)

[5.2 Procedure for CFD Modeling](#)

[5.3 Need for Nondimensional Flow Modeling](#)

[5.4 Flow Over 2D Building and Flow Over an Escarpment](#)

[5.5 Pressure on the Texas Tech University \(TTU\) Building Without Inflow Turbulence](#)

[5.6 Unsteady Flow over Building](#)

[5.7 Flow Around a Cylinder and Practical Relevance to Bridge Aerodynamics](#)

[5.8 Chapter Outcome](#)

[Problems](#)

[References](#)

[6 Advanced Topics](#)

[6.1 Grid Generation for Practical Applications](#)

[6.2 Structural Aeroelasticity and Structural Dynamics](#)

[6.3 Inflow Turbulence by Body Forcing](#)

[6.4 CFD for Improving Wind Turbine Performance and Siting and Wind Tunnel Design](#)

[6.5 Tornado-Structure Interaction](#)

[6.6 Wind Environment Around Buildings](#)

[6.7 Pollutant Transport Around Buildings](#)

[6.8 Parallel Computing for Wind Engineering](#)

[6.9 Chapter Outcome](#)

[References](#)

[7 Introduction to OpenFOAM Application for Wind Engineering \(an Open-Source Program\)](#)

[7.1 Introduction to OpenFOAM and ParaView for Wind Engineering](#)

[7.2 Installation of OpenFOAM, ParaView, and Running a Sample File](#)

[7.3 CFD Solvers and Explanation of Input File for Flow Around a Cube](#)

[7.4 Visualization Using ParaView](#)

[7.5 Analysis of Flow Over Cube Data for Uniform Flow at the Inlet](#)

[7.6 Computation of Turbulent Flow Over a Cube](#)

[7.7 Multilevel Mesh Resolution Using snappyHexMesh Mesh Generator in OpenFOAM](#)

[7.8 Challenges in Using OpenFOAM](#)

[7.9 Summary and Conclusions](#)

[7.10 Chapter Outcome](#)

[References](#)

[Appendix A: Tecplot for Visualization](#)

[Appendix B: Random Process for Wind Engineering](#)

[References](#)

[Appendix C: Direct Solution of \$Ax = b\$ by \$A^{-1}\$](#)

[Index](#)

[End User License Agreement](#)

List of Tables

Chapter 3

[Table 3.1 Comparison of exact derivatives to FDM derivatives and by law of t...](#)

Chapter 4

[Table 4.1 Roughness length \$z_0\$ in meters for different terrain.](#)

Chapter 5

[Table 5.1 Increase in velocity due to escarpment from ASCE 7-16, Table 26.8-...](#)

[Table 5.2 Magnitude of the velocity above the escarpment.](#)

List of Illustrations

Chapter 1

[Figure 1.1 Flow around great Belt East Bridge during flutter condition.](#)

[Figure 1.2 Multiphase flow modeling of liquid droplet impacting a vapor bubb...](#)

[Figure 1.3 Velocity vectors around the roof when a tornado-like vortex coinc...](#)

Chapter 2

[Figure 2.1 Flow around a bridge: Illustration of vortex generation and trans...](#)

[Figure 2.2 Illustration of diffusion and convection.](#)

[Figure 2.3 Flow around circular cylinder: \(a\) inviscid flow has no flow sepa...](#)

[Figure 2.4 Flow around a bluff body \(building\).](#)

[Figure 2.5 Nozzle flow from left to right.](#)

[Figure 2.6 Velocity variation in time in a turbulent flow.](#)

[Figure 2.7 Square pulse plot for \$n = 1, 3, 5, 7,\$ and exact.](#)

[Figure 2.8 Plot \$C_n\$ vs. \$n\$.](#)

[Figure 2.9 Tent function with five points.](#)

[Figure 2.10 Tent function with nine points.](#)

[Figure 2.11 \(a\) Field velocity plot and \(b\) the corresponding spectrum.](#)

[Figure 2.12 Resolved and unresolved frequencies using \(a\) RANS, \(b\) LES, and...](#)

[Figure 2.13 \(a\) Plot of a tent function with a gap for problem 5 and \(b\) plo...](#)

Chapter 3

[Figure 3.1 \(a\) 1D finite difference grid \(b\) 2D finite difference grid.](#)

[Figure 3.2 Symmetric flow in and out of a cavity for a \$4 \times 4\$ grid for hand c...](#)

[Figure 3.3 \(a\) Grid with numbering to form matrix equations \(b\) stream lines...](#)

[Figure 3.4 \(a\) Grid, boundary condition and interior stream function values ...](#)

[Figure 3.5 Optimum relaxation factor RF for \$13 \times 13\$ grid.](#)

[Figure 3.6 Screen run shows the number of iterations for \$RF = 1.6\$.](#)

[Figure 3.7 Flow over a square cylinder or building.](#)

[Figure 3.8 Velocity vector around the cylinder.](#)

[Figure 3.9 Shock wave.](#)

[Figure 3.10 Amplitude of the wave at different times.](#)

[Figure 3.11 Comparison of an exact sine wave with the FDM method after two c...](#)

[Figure 3.12 Wave profile after 2-time units. \(a\) Using CN method, \(b\) using ...](#)

[Figure 3.13 Staggered and nonstaggered storage system for cell-centered grid...](#)

[Figure 3.14 Storage of the variables at the nodes and cell centered.](#)

[Figure 3.15 Unstructured grid.](#)

[Figure 3.16 \(a\) Structured grid numbering. \(b\) Unstructured grid numbering....](#)

[Figure 3.17 Storage position for the A matrix in the unstructured grid syste...](#)

Chapter 4

[Figure 4.1 Wind profile for \(a\) straight-line boundary layer wind, \(b\) thund...](#)

[Figure 4.2 Mean velocity profile over different ground roughness.](#)

[Figure 4.3 Speed-up due to wind flow over a hill.](#)

[Figure 4.4 Gable and hip roof.](#)

[Figure 4.5 Effect of wind on rigid \(high frequency\) and flexible structure \(...\)](#)

[Figure 4.6 Vortex shedding behind a circular cylinder.](#)

[Figure 4.7 Time variation of drag \(\$C_d\$ \) and lift \(\$C_l\$ \) force coefficients.](#)

[Figure 4.8 Lift versus angle of attack for square, rectangle, and half circl...](#)

[Figure 4.9 Aerodynamic damping: \(a\) positive and \(b\) negative.](#)

[Figure 4.10 Wind flow over a building.](#)

Chapter 5

[Figure 5.1 Comparison of field and wind tunnel pressure coefficients: \(a\) Si...](#)

[Figure 5.2 Lack of energy in the WT wind spectrum compared to filed measur...](#)

[Figure 5.3 Boundary conditions for 2D flow over obstacle.](#)

[Figure 5.4 Illustration of KH array numbers for obstacles modeling.](#)

[Figure 5.5 Flow region with building.](#)

[Figure 5.6 Velocity contour with pressure values as the color for velocities...](#)

[Figure 5.7 \(a\) Close-up vector plot and \(b\) pressure contour lines with valu...](#)

[Figure 5.8 Flow over an escarpment.](#)

[Figure 5.9 U velocity contour plot.](#)

[Figure 5.10 V velocity contour plot.](#)

[Figure 5.11 Velocity with height for CFD and ASCE.](#)

[Figure 5.12 Computational region with boundary conditions.](#)

[Figure 5.13 Plan and elevation of the computational region shown in H.](#)

[Figure 5.14 Identifying building location nodes.](#)

[Figure 5.15 Illustration of points where pressure is recorded in time on the...](#)

[Figure 5.16 Plot from **yif-o.plt** file or time variation of pressure.](#)

[Figure 5.17 Recorded \$C_p\$ statistics along the centerline of the building.](#)

[Figure 5.18 Mean, max, and min pressure coefficients along the centerline.](#)

[Figure 5.19 CFD pressure coefficient comparison with WT50 and WT6 measuremen...](#)

[Figure 5.20 3D pressure variation around the building.](#)

[Figure 5.21 Velocity magnitude plot as isosurface for \(a\) 1.35 and \(b\) 0.31....](#)

[Figure 5.22 Velocity vector plot for \(a\) elevation and \(b\) plan view.](#)

[Figure 5.23 Zoomed velocity vector plot for \(a\) elevation and \(b\) plan view....](#)

[Figure 5.24 Close-up view of velocity vector plot with pressure contour.](#)

[Figure 5.25 Sidewalls and roof from 3D are shown in 2D plane.](#)

[Figure 5.26 Pressure coefficient \$C_p\$ on sidewalls and roof. \(a\) Mean, \(b\) min...](#)

[Figure 5.27 Wind spectrum with respect to LES.](#)

[Figure 5.28 Spurious pressure reduction: \(a\) \$f_{\max} = 4\$ and \(b\) \$f_{\max} = 10\$.](#)

[Figure 5.29 Variation of U velocity at inlet and building location and press...](#)

[Figure 5.30 Wind spectrum: \(a\) at the inlet and \(b\) at the building location...](#)

[Figure 5.31 Pressure variation on building in time: \(a\) full view and \(b\) cl...](#)

[Figure 5.32 Mean, max, and min pressure coefficients along the centerline.](#)

[Figure 5.33 CFD pressure coefficient in comparison with WT50 and WT6 measure...](#)

[Figure 5.34 Peak \$C_p\$ for \$f_{\min} = 0.1\$.](#)

[Figure 5.35 Velocity spectrum at the inlet using 100 time unit data.](#)

[Figure 5.36 Isosurface plot.](#)

[Figure 5.37 Plot along the centerline of the building \(a\) vector plot and \(b...](#)

[Figure 5.38 Plan view of the building at \$K = 5\$.](#)

[Figure 5.39 Pressure plot on the roof \(a\) without contour lines and \(b\) with...](#)

[Figure 5.40 Mean pressure coefficients \(\$C_{p\text{mean}}\$ \) on all the surfaces of the T...](#)

[Figure 5.41 Minimum and maximum peak pressure coefficients on sidewalls and ...](#)

[Figure 5.42 Close-up view of flow around a circular cylinder for a \$41 \times 61\$ g...](#)

[Figure 5.43 Flow over a square cylinder problem.](#)

[Figure 5.44 Flow over square cylinder grid generation definitions for **rg.f**...](#)

[Figure 5.45 Drag \(\$C_d\$ \) and lift \(\$C_l\$ \) coefficient versus time.](#)

[Figure 5.46 Contour and vector Plots around the square cylinder \(a\) contour ...](#)

[Figure 5.47 Stream traces plot.](#)

Chapter 6

[Figure 6.1 Grid generation for flow around complex building using snappyHexM...](#)

[Figure 6.2 Flow around complex building using OpenFOAM: velocity contour plo...](#)

[Figure 6.3 Aeroelastic interaction of wind on structures \(a\) response due to...](#)

[Figure 6.4 Response of the GBEB for \(a\) \$U^* = 1.2\$ and \(b\) \$U^* = 1.45\$.](#)

[Figure 6.5 Flow around the GBEB bridge for \$U^* = 12.5\$ \(a\) full view of the br...](#)

[Figure 6.6 Flow around GBEB for \$U^* = 1.45\$ \(flutter condition\).](#)

[Figure 6.7 Different methods to model a fan or turbine \(a\) fan or turbine, \(...](#)

[Figure 6.8 Tornado paths with respect to a hill \(a\) different paths and \(b\) ...](#)

[Figure 6.9 Tornado-hill interaction for angle 15 degree. \(a\) Vortex at diffe...](#)

[Figure 6.10 \(a\) Stationary vortex chamber. \(b\) Moving vortex chamber.](#)

[Figure 6.11 \(a\) TTU tornado chamber. \(b\) Simplified geometry for CFD model o...](#)

Chapter 7

[Figure 7.1 Details of **building** data or case file.](#)

[Figure 7.2 Elevation and plan of the computational region.](#)

[Figure 7.3 \(a\) 3D view of the computational domain with axes and \(b\)_grid sp...](#)

[Figure 7.4 Detail of file “transportProperties” under **constant** directory.](#)

[Figure 7.5 Detail file “U” for initial conditions under **0** directory.](#)

[Figure 7.6 Detail file “p” for initial conditions under **0** directory.](#)

[Figure 7.7 \(a\) Bottom-level vertices number at \$z = 0\$ and block numbers. \(b\) ...](#)

[Figure 7.8 Detail file “blockMeshDict” for initial conditions under **system** d...](#)

[Figure 7.9 Detail file “fvSchemes” for initial conditions under **system** direc...](#)

[Figure 7.10 Detail file “fvSolution” for initial conditions under **system** dir...](#)

[Figure 7.11 Detail of “controlDict” file for initial conditions under **system**](#)

[Figure 7.12 Time variation of pressure close to the windward edge of the roo...](#)

[Figure 7.13 3D view of the computational region box.](#)

[Figure 7.14 Pressure contour at \$y = 3.5\$.](#)

[Figure 7.15 \(a\) Close-up view with pressure as contour color and \(b\) close-u...](#)

[Figure 7.16 Streamline plot for xz slice.](#)

[Figure 7.17 Variation of pressure and velocity on the roof of the cube along...](#)

[Figure 7.18 Details of **buildingLes1** data or case file.](#)

[Figure 7.19 List of “turbulenceProperties” file.](#)

[Figure 7.20 List of “controlDict” file.](#)

[Figure 7.21 List of “fvSchemes” file.](#)

[Figure 7.22 List of “fvSolution” file.](#)

[Figure 7.23 List of “nut” file.](#)

[Figure 7.24 View of the inlet velocity profile.](#)

[Figure 7.25 Time variation of the pressure on the roof \(a\) using “bounded Ga...](#)

[Figure 7.26 Multilevel complex grid generation illustration using three leve...](#)

[Figure 7.27 Details of the cube with origin.](#)

[Figure 7.28 Listing of “meshQualityDict” file.](#)

[Figure 7.29 Listing of “surafceFeaturesDict” file.](#)

[Figure 7.30 Listing of “snappyHexMesh” file.](#)

[Figure 7.31 Comparison of pressure contour for \(a\) Level 3 mesh and \(b\) Leve...](#)

[Figure 7.32 Time variation of pressure at probing points 5 to 9 from \(a\) Lev...](#)

Appendix B

[Figure B.1 Autocorrelation function and integral time scale.](#)

Computational Fluid Dynamics for Wind Engineering

R. Panneer Selvam, Ph.D., P.E.

University Professor

Department of Civil Engineering

University of Arkansas, Fayetteville, AR, USA

WILEY Blackwell

This edition first published 2022
© 2022 John Wiley & Sons Ltd

All rights reserved. No part of this publication may be reproduced, stored in a retrieval system, or transmitted, in any form or by any means, electronic, mechanical, photocopying, recording or otherwise, except as permitted by law. Advice on how to obtain permission to reuse material from this title is available at <http://www.wiley.com/go/permissions>.

The right of R. Panneer Selvam to be identified as the author of this work has been asserted in accordance with law.

Registered Office(s)

111 River Street, Hoboken, NJ 07030, USA

The Atrium, Southern Gate, Chichester, West Sussex, PO19 8SQ, UK

Editorial Office

9600 Garsington Road, Oxford, OX4 2DQ, UK

For details of our global editorial offices, customer services, and more information about Wiley products visit us at www.wiley.com.

Wiley also publishes its books in a variety of electronic formats and by print-on-demand. Some content that appears in standard print versions of this book may not be available in other formats.

Limit of Liability/Disclaimer of Warranty

In view of ongoing research, equipment modifications, changes in governmental regulations, and the constant flow of information relating to the use of experimental reagents, equipment, and devices, the reader is urged to review and evaluate the information provided in the package insert or instructions for each chemical, piece of equipment, reagent, or device for, among other things, any changes in the instructions or indication of usage and for added warnings and precautions. While the publisher and authors have used their best efforts in preparing this work, they make no representations or warranties with respect to the accuracy or completeness of the contents of this work and specifically disclaim all warranties, including without limitation of any implied warranties of merchantability or fitness for a particular purpose. No warranty may be created or extended by sales representatives, written sales materials, or promotional statements for this work. The fact that an organization, website, or product is referred to in this work as a citation and/or potential source of further information does not mean that the publisher and authors endorse the information or services the organization, website, or product may provide or recommendations it may make. This work is sold with the understanding that the publisher is not engaged in rendering professional services. The advice and strategies contained herein may not be suitable for your situation. You should consult with a specialist where appropriate. Further, readers should be aware that websites listed in this work may have changed or disappeared between when this work was written and when it is read. Neither the publisher nor authors shall be liable for any loss of profit or any other

commercial damages, including but not limited to special, incidental, consequential, or other damages.

Library of Congress Cataloging-in-Publication Data

Name: Selvam, R. Panneer, author.

Title: Computational fluid dynamics for wind engineering / R. Panneer Selvam.

Description: Hoboken, NJ : Wiley-Blackwell, 2022. | Includes bibliographical references and index.

Identifiers: LCCN 2022012496 (print) | LCCN 2022012497 (ebook) | ISBN 9781119845058 (cloth) | ISBN 9781119845065 (adobe pdf) | ISBN 9781119845072 (epub)

Subjects: LCSH: Wind-pressure. | Computational fluid dynamics.

Classification: LCC TA654.5 .S4395 2022 (print) | LCC TA654.5 (ebook) | DDC 624.1/75—dc23/eng/20220624

LC record available at <https://lcn.loc.gov/2022012496>

LC ebook record available at <https://lcn.loc.gov/2022012497>

Cover Design: Wiley

Cover Image: © HelloRF [Zcool/Shutterstock.com](https://www.shutterstock.com)

Preface

My computational fluid dynamics (CFD) for wind engineering journey started around January 1983 at Texas Tech University (TTU) when myself and Dr. Kishor Mehta were brainstorming on new research areas on a Saturday morning and what I can consider for my PhD topic. Before that, I did not know anything about CFD and not much in fluid mechanics except taking a four-semester course work in my undergraduate program. Since I had reasonable background on numerical methods and its application to solid mechanics from my master's work in India and in the United States, I decided to apply those concepts to wind engineering applications. Especially, the tornado force on building fascinated me because only after I came to Lubbock, TX, I came to know about tornado and its devastation. In India where I grew up, I was exposed to hurricane-type wind extensively, and this may be another reason for me getting into wind engineering research area. At that time, I did not realize what I was getting into. Dr. Mehta did say I might not realize my dream even after 80 years old. However, Dr. James McDonald (my advisor) and Dr. Kishor Mehta did support my idea, and I started to apply numerical methods in fluid mechanics for tornado forces on buildings. I did not do any substantial work in my PhD work, but it did open the CFD application for wind engineering research area. My next vertical advancement happened when I visited Commonwealth Scientific and Industrial Research Organization (CSIRO), Australia, as a research scientist to work under Dr. John Holmes during the summer of 1990. He is a fun and nice person to work with, and I am glad he gave me an opportunity to work on CFD application to thunderstorm downdraft modeling. There I met Dr. David Peterson, and he taught me the

implementation of the SIMPLE method of solving the Navier-Stokes (NS) equations and law of the wall boundary condition. There I used CFD to compute velocity in a thunderstorm downdraft and flow over 3D building using $k-\epsilon$ turbulence model. The paper (Selvam and Holmes [1992](#)) becomes the beginning of thunderstorm downdraft study in wind engineering. From there on different challenges in CFD for wind engineering were resolved and now we are in a much better situation for application in wind engineering.

Dr. Allan Larsen in 1998, Dr. Partha Sarkar in 2010, and Dr. Prem Krishna in 2002, 2008, and 2017 requested me to write review papers on CFD for wind engineering. Those experiences gave me chances to reflect and advance myself for further developments. In the recent years, Dr. Arindam Chowdhury from Florida International University has become another motivator to expand my journey. Dr. Chowdhury and his student Dr. M. Moravej provided me wind tunnel data for the 1:6 scale TTU building, and he explained to me the partial turbulence simulation (PTS) method reported in Mooneghi et al. (2016) paper. This helped me to learn more about turbulence effects on building and challenges in wind tunnel modeling. He is a great person, and he opened my mind to learn more about inflow turbulence generation methods and energy cascade in turbulence. This is a concept many did not apply in turbulence modeling. If this concept were understood for practical application, the CFD application would have progressed much quicker. Murakami et al. ([1987](#)) used recycling method of considering turbulence in the flow using large eddy simulation (LES) for the first time in wind engineering. The recycling method has been used in many applications for several years after that. I also tried to implement it and reported my findings in Selvam ([1997](#)), and I thought at that time the turbulence energy has to be maintained as time goes on. From the numerical

experiment, I found that after some time, most of the turbulence energy got lost in the computation. This could be due to the numerical diffusion as well as the energy cascade phenomenon. Because of my ignorance, I did not report the details in any of my publications. In recent years, I learnt that because of energy cascade and 3D modeling, the energy from lower frequency is transferred to higher frequency and also the waves get stretched and twisted.

In this work, random Fourier-based inflow turbulence generation method is used as inflow in [Chapter 5](#) and the peak pressure on building is computed. The program developed for this case can be used for building aerodynamics study without inflow and with inflow. This helps the student to learn the power of CFD to some extent. This tool also gives a chance for students to generate their own wind data and analyze them for wind spectrum. The other notable problem considered is the vortex shedding in 2D cylinders. This provides a pathway to understand the vortex-induced vibration (VIV) issues in thin structures and bridges. The program for that also is used for class instruction. The programs developed for this class can run on a personal computer, and this makes it easier for students to use. The outputs are written in a format suitable for tecplot visualization program. The open-source visualization programs like ParaView can be used, and it is not user-friendly. However, the data can be manipulated for other systems easily because the files are in ASCII format.

To perform CFD modeling for building and bridge aerodynamics, some understanding of the NS equation, properties of turbulence, turbulence modeling, introduction to finite difference method, and wind engineering is necessary, and they are introduced briefly in [Chapters 1-4](#). At the end of each chapter, necessary homework problems by hand or computers are provided to have hands-on experience.

A brief review of CFD application in wind engineering is provided in [Chapter 6](#). I do apologize to many researchers whose work I could not include in [Chapter 6](#) due to lack of time and space. In [Chapter 7](#), use of OpenFOAM for wind engineering is introduced.

This course material was developed in the summer of 2020 to teach in the fall semester. Before the Fall of 2020, I taught CFD class twice, which helped me to develop the course material more focused toward wind engineering. The material for the class was expanded as the courses were taught. I had few fresh graduate students like Ms. Kaley Collins, Mr. Caleb Chestnut, and Mr. Gerardo Aguilar who gave a lot of support to teach this class in addition to my graduate students (Mr. Sumit Verma and Ms. Zayuris Atencio). Because of them, I got Mr. Andrew Deschenes, Mr. Wesley Keys, and Mr. Yancy Schrader in my class as students. The participation of all of them really improved the course material.

Even though the course material is more toward wind engineering application, if someone wants to write their own program, numerical algorithms are provided and several programs are listed for their own development.

The course was taught in the Fall of 2020 with our own CFD research code and tecplot up to [Chapter 5](#). The students ran the programs on personal computer, and that made it easier for students. The visualization program tecplot is user-friendly, but it is a commercial program. If someone wants to teach the [Chapter 5](#) material using open-source CFD program OpenFOAM and open-source visualization program ParaView, they can do so by using the material in [Chapter 7](#). The major challenge may be to adopt an inflow turbulence generator available from OpenFOAM.

Since no other textbook on computational wind engineering is available at this time, I developed a teaching philosophy after several months of reflection. If you have any comments for improvement after going over the material, please email it to me. This means a lot and I greatly appreciate. I do hope this material is useful for students, industry practitioners, and researchers. I would like to thank Dr. A. Chowdhury for going over the material and providing valuable comments for improvement. Finally, I like to acknowledge the financial support received from Airforce, Navy, NASA, NSF, FHWA, James T. Womble Professorship and the Department of Civil Engineering, University of Arkansas over the years to conduct many of the research work reported in this book.

References

- Murakami, S., Mochida, A., and Hibi, K. (1987). Three-dimensional numerical simulation of airflow around a cubic model by means of large eddy simulation. *Journal of Wind Engineering and Industrial Aerodynamics* 25: 291-305.
- Mooneghi, M.A., Irwin, P., and Chowdhury, A.G. (2016). Partial turbulence simulation method for predicting peak wind loads on small structures and building appurtenances. *Journal of Wind Engineering and Industrial Aerodynamics*. 157: 47-62.
- Selvam, R.P. (1997). Computation of pressures on Texas Tech Building using large eddy simulation. *Journal of Wind Engineering and Industrial Aerodynamics* 67 & 68: 647-657.
- Selvam, R.P. and Holmes, J.D. (1992). Numerical simulation of thunderstorm downdrafts. *Journal of Wind*

Engineering and Industrial Aerodynamics 44: 2817-2825.

R. Panneer Selvam
University of Arkansas
September, 2021

1

Introduction

Fluid mechanics and heat transfer have extensive application. From aeronautical industry to automatic industry, it is applied to several areas. Some of the notable areas are:

1. Aeronautical industry - design of airplane to electronic devices
2. Automobile industry
3. Building and bridge aerodynamics (Selvam [2017](#))
4. Electronic cooling (Silk et al. [2008](#); Sarkar and Selvam [2009](#))
5. Environmental flow and heat transfer
6. Metrological flow and weather prediction
7. Hydraulic flow
8. Water treatment (Liu and Zhang [2019](#))
9. Wind energy

In all areas, computer modeling has been extensively used in the recent years, and this branch of computation is called computational fluid dynamics (CFD). CFD provides the detail of velocities, pressure, and temperature at every point at each time in the computational domain. This helps to create animation in time and provides the detail of the flow changes in time. To gather this much of information from experiment is very expensive. In certain situation like weather prediction, we cannot do any experiment and computer simulation is the only tool to predict the weather.

The major challenge in CFD is to develop a reliable computer model for a particular application. If this is established for a particular application, it will be very useful in the design of the system.

The CFD is applied from single-phase flow to multiphase flow. In the multiphase flow, it can be liquid-vapor flow, solid-liquid flow, and solid-liquid-vapor flow. In these flows, chemical reactions can occur. Some of the challenging flows I encountered in the past 30 years are

Wind-bridge interaction: Here the bridge moves due to wind and hence beyond certain velocities the bridge can flutter as reported in Selvam et al. ([2002](#)). Below the critical velocity for flutter, the bridge will not have unlimited oscillations. The concept of moving grid has to be used in addition to regular CFD modeling. The Tacoma Narrow Bridge failed due to flutter for a velocity of 64 km/h (17.8 m/s) in 1940. The critical velocity for flutter for Great Belt East Bridge is 252 km/h (70 m/s) as reported in Selvam et al. ([2002](#)). The critical velocity depends upon the shape and structural properties of the bridge. The flow features during flutter condition are shown in [Figure 1.1](#).

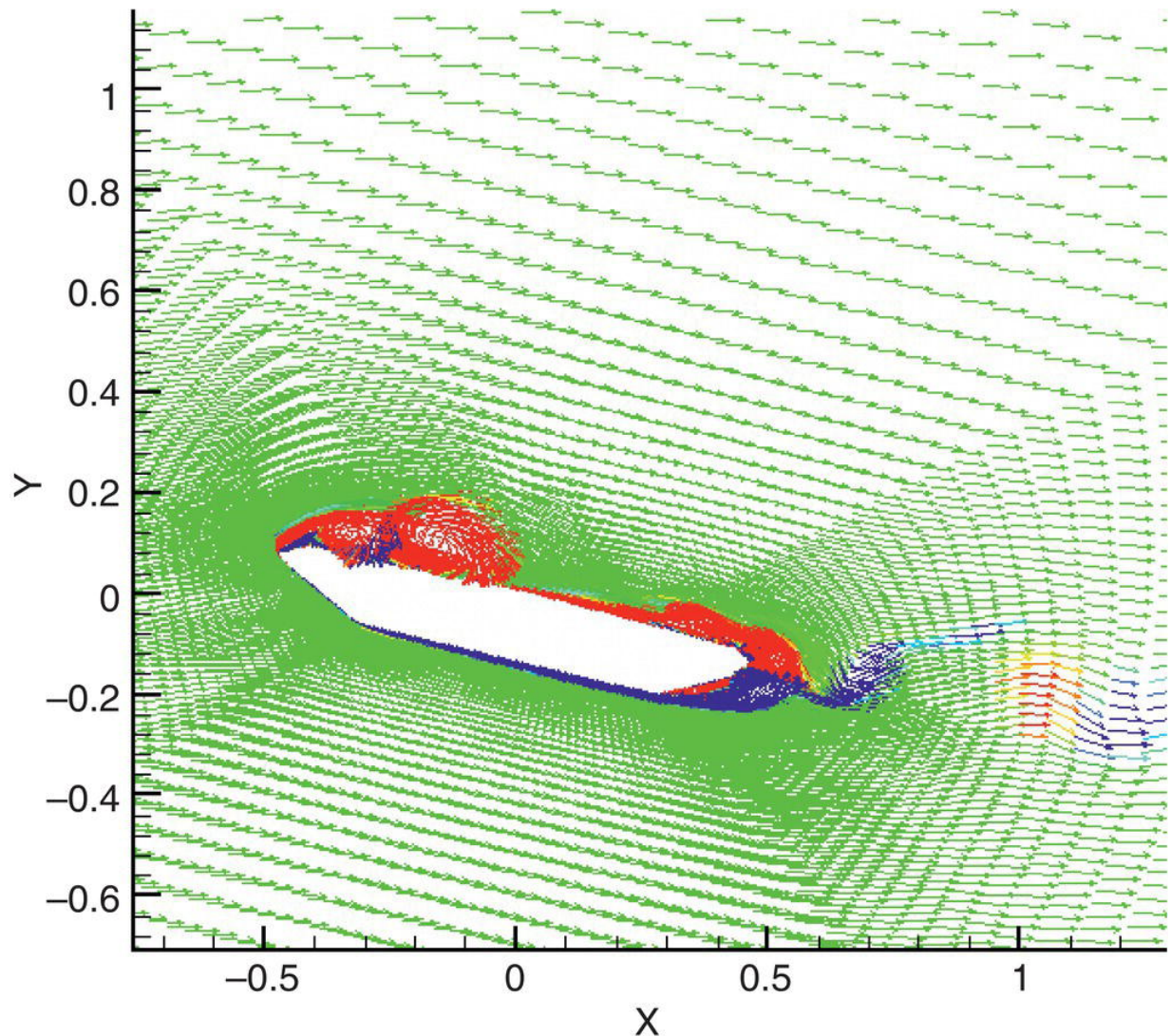


Figure 1.1 Flow around great Belt East Bridge during flutter condition.

Heat transfer mechanism in spray cooling: Here, when a liquid droplet impacts a hot plate with a bubble growing in a thin liquid film; heat is removed due to complex interaction of droplet impact and vapor bubble. This high heat removal phenomena are explained in Selvam et al. (2006). For this, multiphase flow modeling of liquid and vapor is considered. In [Figure 1.2](#) the liquid and vapor phases before the droplet impacts a vapor bubble in a liquid film are shown.

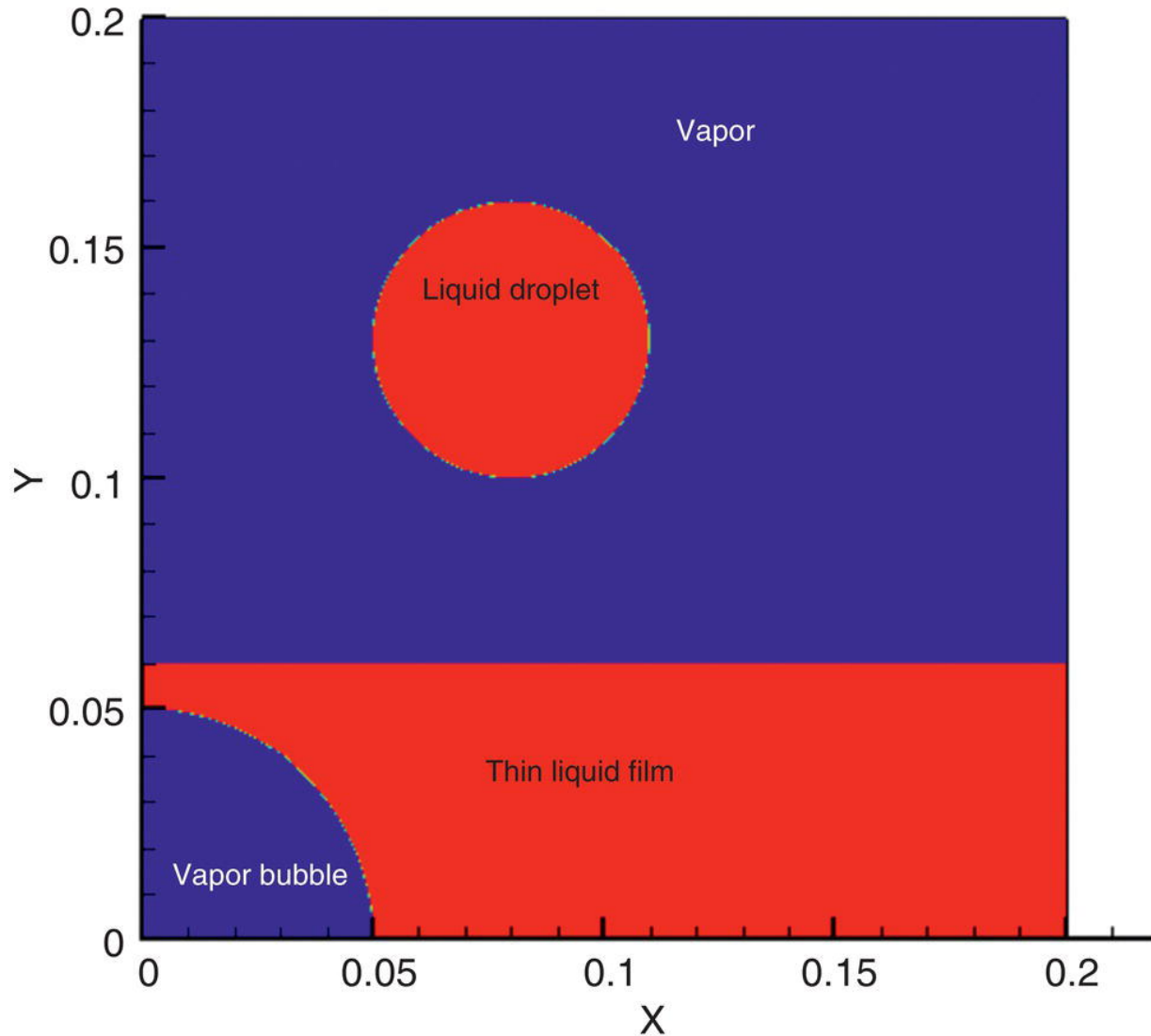


Figure 1.2 Multiphase flow modeling of liquid droplet impacting a vapor bubble in liquid film.

Tornado-building interaction: This study is reported in Selvam and Millett ([2003](#), [2005](#)). Here in a tornadic flow how a roof of a building is lifted up is explained using CFD. [Figure 1.3](#) shows the velocity vector over the roof when a tornado-like vortex coincides with the center of a cubical building.

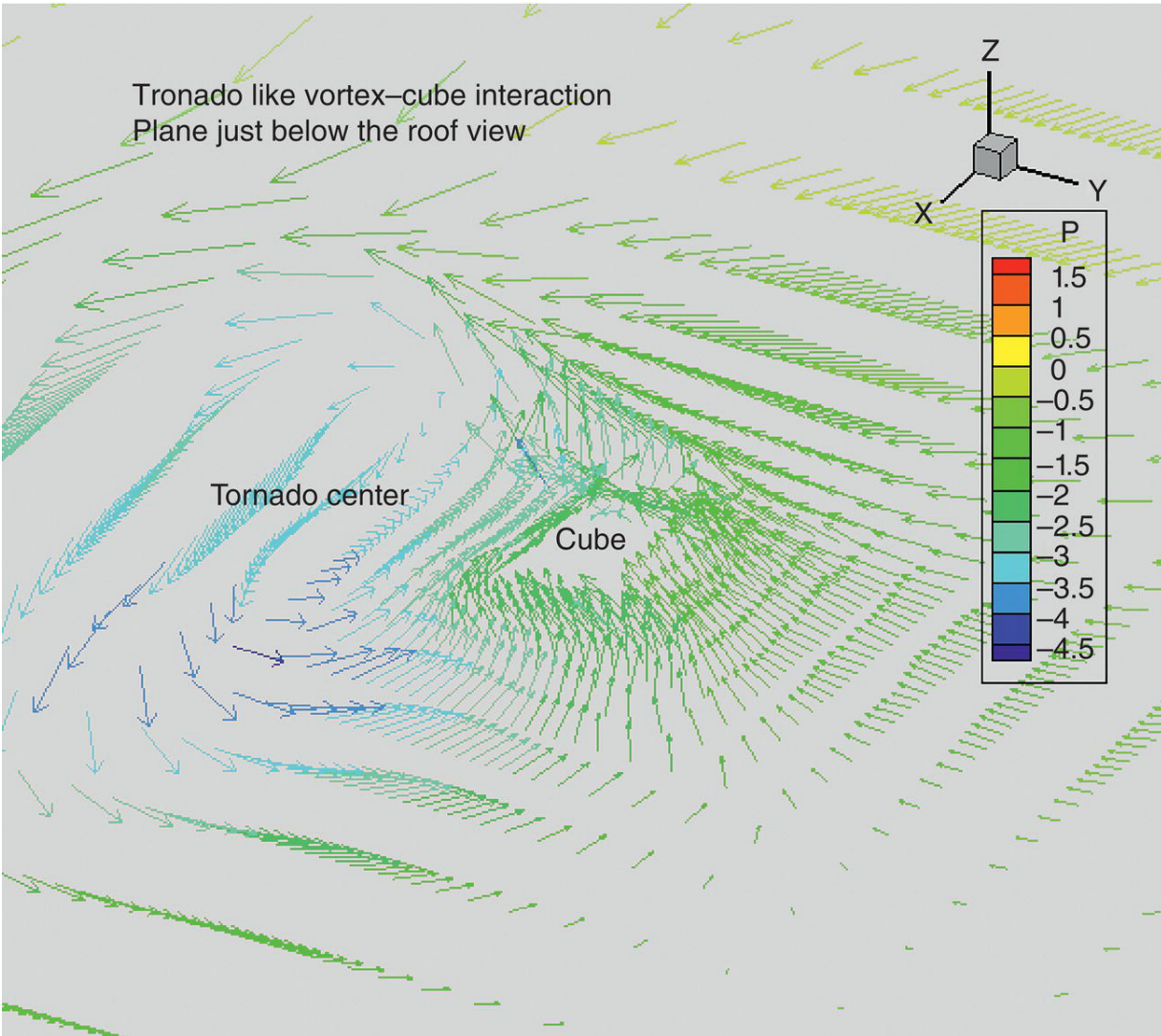


Figure 1.3 Velocity vectors around the roof when a tornado-like vortex coincides with the center of a cubical building.

1.1 Brief Review of Steps in CFD Modeling

In the CFD modeling, the steps are very similar to well-established solid mechanics modeling. The major differences being most of the CFD applications are nonlinear and hence several iterations or time steps need to be performed.

Step 1: Grid Generation or Preprocessing: This may be the most time-consuming part if one has a complicated domain. If simple domain where in rectangular grid systems can be used, then the grid generation may be an easier task. Still one has to focus on the grid refinements in the boundary layer and in the regions of steep flow. Also, one has to make sure that grid spacing variation should not be high. The preferred ratio is 1.0–1.5. Very large ratios like more than 5 or 10 are not preferable. For this step, extensive grid generation programs were developed in the recent years.

Step 2: Flow Solver: Once the grid is generated for a particular problem and the proper initial and boundary conditions are given for the problem, one can solve the Navier–Stokes (NS) equations. This is the most computer time-intensive step. For this several methods from direct to iterative procedures are developed to solve the $Ax = b$ equations. To reduce computer time, high performance or parallel computing is also utilized. Sarkar and Selvam (2009) utilized parallel computing to reduce the computer time from 50 to 3 days for spray cooling applications. They also compared the performance of different iterative solvers in the parallel computing environment.

Step 3: Postprocessing: In this step, the output from flow solver is processed to mine valuable information. Here this can be done by regular x–y graphs, contours, vector plots, and the combination of all. If the data is written for several time steps for the whole region, one can make animation using software like TECPLOT, and flow features can be investigated. The flow visualization technique is very sophisticated and some time it is an art than science.

If it is a design, then one can change the parameters of the flow variable or computational domain and further computer runs can be made for further investigations.

Benefits of CFD:

1. Data available for all points in space and time.
2. Inexpensive comparing to experiment. Especially with the developments in computer speed and memory, CFD programs can run in a personal computer. The major hurdle is validating the CFD with experiment to have reliability.
3. Visualization and animation of data to understand the physical problem is easy to implement. This helps anyone to understand complex fluid phenomena.

1.2 CFD for Wind Engineering or Computational Wind Engineering

In wind engineering, the loads on building and bridges are obtained from wind tunnel (WT) measurements or field measurements. The field measurement is very expensive and only very limited field studies are conducted like Texas Tech University building. Currently, WT is the major tool used to investigate forces on buildings and to develop code regulations like ASCE 7-16. In recent years, CFD is emerging as an alternate tool. For more than 30 years, different researchers raised its capabilities and slowly it is becoming a reasonable tool to be used in wind engineering because of the availability of high-performance computers with large storage capacities. The work reported by Selvam ([1992](#)) took more than a day for one computer run. With the current computer capabilities, one can solve the same problem in few minutes. Hence, the speed increased may be more than 100 times in a single processor. With multiple processors, we can increase the speed at least 10 times. If the CFD model is well validated with experiments, then it becomes the most economical tool compared to